Vol 17 No 8, August 2008
1674-1056/2008/17(08)/2837-07

Chinese Physics B

© 2008 Chin. Phys. Soc.
and IOP Publishing Ltd

# The characteristics of nonlinear chaotic dynamics in quantum cellular neural networks*

Wang Sen(王 森)[a], Cai Li(蔡 理)[a], Kang Qiang(康 强)[b],
Wu Gang(吴 刚)[a], and Li Qin(李 芹)[a]

[a] *The Science Institute, Air Force Engineering University, Xi'an 710051, China*

[b] *Science Research Department, Air Force Engineering University, Xi'an 710051, China*

(Received 16 October 2007; revised manuscript received 13 November 2007)

With the polarization of quantum-dot cell and quantum phase serving as state variables, this paper does both theoretical analysis and simulation for the complex nonlinear dynamical behaviour of a three-cell-coupled Quantum Cellular Neural Network (QCNN), including equilibrium points, bifurcation and chaotic behaviour. Different phenomena, such as quasi-periodic, chaotic and hyper-chaotic states as well as bifurcations are revealed. The system's bifurcation and chaotic behaviour under the influence of the different coupling parameters are analysed. And it finds that the unbalanced cells coupled QCNN is easy to cause chaotic oscillation and the system response enters into chaotic state from quasi-periodic state by quasi-period bifurcation; however, the balanced cells coupled QCNN also can be chaotic when coupling parameters is in some region. Additionally, both the unbalanced and balanced cells coupled QCNNs can possess hyper-chaotic behaviour. It provides valuable information about QCNNs for future application in high-parallel signal processing and novel ultra-small chaotic generators.

**Keywords:** quantum cellular neural network, bifurcation, chaos, quantum cellular automata
**PACC:** 0545, 7450

## 1. Introduction

For nearly 40 years the microelectronics industry has enjoyed dramatic improvements in the speed and size of electronic devices. Adherence to these fast improvements has been a monumental task requiring rapid improvements in all aspects of integrated circuit fabrication to permit manufacturers to both shrink the size of devices, and increase chip size. As device sizes decrease continually, the physical limitations of conventional electronics including power consumption, interconnection, and lithography become increasingly difficult to surmount.[1] Studies indicate that as early as 2019, the Complementary Metal Oxide Semiconductor (CMOS) transistor may hit physical scaling limits that inhibit this aggressive packing of devices. However, these obstacles may provide an opportunity for alternative device technologies designed for the nanometre regime and interconnected in an appropriate architecture.

One such device, proposed by Lent *et al* is Quantum-Dot Cellular Automata (QCA).[2−4] which employs arrays of coupled quantum dots to transfer information by the propagation of polarized charge, rather than the flow of current. The advantages of QCA lie in the extremely high packing densities possible due to the small size of the dots, the simplified interconnection, and the extremely low power consumption. QCA can be applied to digital circuits[5−7] and analog circuits. One of analog application is Quantum cellular Neural Network (QCNN)[8−12] based on the Schrödinger equation in which cells composed of interacting quantum-dots are employed in Cellular Neural Network (CNN) architecture.[13]

QCNNs represent an innovative architecture for massive signal processing and exhibit interesting spatiotemporal phenomena.[14] One of their peculiarities lies in the further degree of freedom possessed by each cell due to quantum interaction between dots. This fact makes QCNNs possess the complicated dynamical behaviours because of the physical interaction between quantum dots. In this paper, we study the complex chaotic dynamical behaviour of a three-cell-coupled QCNN,[10] including equilibrium points, bifurcations,[15] and chaotic behaviours; analyse the

*Project supported by the Natural Science Foundation of Shaanxi Province, China (Grant No 2005F20) and the Innovation Funds of the College of Science, Air Force University of Engineering (2007B003).

QCNN's bifurcations and chaotic behaviours under the influence of the different coupling parameters; and find that the QCNN includes plenty of quasi-periodic, chaotic and hyper-chaotic behaviours.[16,17] The study we will discuss could be very important for future ultra-small realization and application of CNNs.

## 2. Dynamic model of the QCNN

QCNNs are composed of local coupled QCAs. A basic QCA consists of four quantum dots in a square array coupled by tunnel barriers. Figure 1(a) shows a ring constructed by four single electron tunnel junctions and four quantum dots located at the corners. If it contains two electrons hopping among the four quantum dots, it becomes a QCA cell. Electrons can tunnel between the quantum dots in the same cell through tunnel junctions. The electrons tend to occupy antipodal sites within the cell due to their mutual electrostatic repulsion, thus an isolated cell possesses two completed polarized states as shown in Fig.1(b).

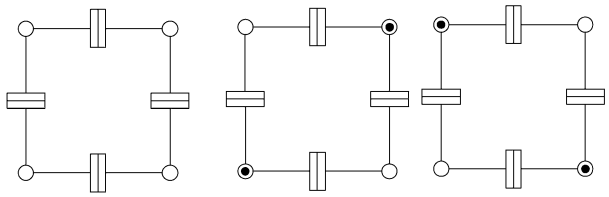



**Fig.1.** Schematic diagram of QCA cell: (a) the ring constructed by four tunnel junctions and four quantum dots; (b) the two complete polarization state of QCA cell.

A QCNN can be described by a set of state variables which contain the classical cell polarization $P$ and a quantum mechanical phase angle $\varphi$. Denoted by $P_i$ the $i$th cell polarization and by $\varphi_i$ the phase angle, we characterize the three-cell coupled QCNN by the presence of three quantum variables $\varphi_1$, $\varphi_2$, and $\varphi_3$ in addition to the macroscopic degrees of freedom $P_1$, $P_2$, and $P_3$.

In its general form, the model of the three-cell coupled QCNN can be described by the following state equation:[10]

$$\begin{aligned}
\frac{\mathrm{d}P_1}{\mathrm{d}t} &= -2b_1\sqrt{1-P_1^2}\sin\varphi_1,\\
\frac{\mathrm{d}\varphi_1}{\mathrm{d}t} &= -w_1(P_1-P_2-P_3)+2b_1\frac{P_1}{\sqrt{1-P_1^2}}\cos\varphi_1,\\
\frac{\mathrm{d}P_2}{\mathrm{d}t} &= -2b_2\sqrt{1-P_2^2}\sin\varphi_2,\\
\frac{\mathrm{d}\varphi_2}{\mathrm{d}t} &= -w_2(P_2-P_1-P_3)+2b_2\frac{P_2}{\sqrt{1-P_2^2}}\cos\varphi_2,\\
\frac{\mathrm{d}P_3}{\mathrm{d}t} &= -2b_3\sqrt{1-P_3^2}\sin\varphi_3,\\
\frac{\mathrm{d}\varphi_3}{\mathrm{d}t} &= -w_3(P_3-P_2-P_1)+2b_3\frac{P_3}{\sqrt{1-P_3^2}}\cos\varphi_3, \quad (1)
\end{aligned}$$

where $b_1$, $b_2$, and $b_3$ are proportional to the inter-dot energy inside each cell (for identical cells $b_1 = b_2 = b_3$) and $w_1$, $w_2$, and $w_3$ weight the effects on the cell of the difference of polarization of the neighbouring cells (like the A cloning templates in traditional CNNs).

## 3. Numerical calculation and analysis

The numerical calculation is based on the state equation (1), and the range of parameters are $b_i > 0$, ($i$=1, 2, 3) and $w_i > 0$, ($i$=1, 2, 3).

### 3.1. Equilibrium points

The equilibrium points are given by

$$\begin{aligned}
&-2b_1\sqrt{1-P_1^2}\sin\varphi_1 = 0,\\
&-w_1(P_1-P_2-P_3)+2b_1\frac{P_1}{\sqrt{1-P_1^2}}\cos\varphi_1 = 0,\\
&-2b_2\sqrt{1-P_2^2}\sin\varphi_2 = 0,\\
&-w_2(P_2-P_1-P_3)+2b_2\frac{P_2}{\sqrt{1-P_2^2}}\cos\varphi_2 = 0,\\
&-2b_3\sqrt{1-P_3^2}\sin\varphi_3 = 0,\\
&-w_3(P_3-P_2-P_1)+2b_3\frac{P_3}{\sqrt{1-P_3^2}}\cos\varphi_3 = 0. \quad (2)
\end{aligned}$$

When $\varphi_1$, $\varphi_2$, $\varphi_3 \in [0\ \pi]$, all the equilibrium points [$P_1$, $P_2$, $P_3$, $\varphi_1$, $\varphi_2$, $\varphi_3$] have the form [$P_1$, $P_2$, $P_3$, $0, 0, 0$]. Due to the complexity of equilibrium point expression, the equilibrium values have been evaluated numerically on a predefined grid of parameters as shown in Table 1. Here we let $b_1 = b_2 = b_3 = b$ and $w_1 = w_2 = w_3 = w$.

From the Table 1, we can know that the equilibrium points are centrosymmetric, verified by the fact that the left hand side of Eq.(2) is an odd function.

From Eq.(2), it also can be known that the origin (0, 0, 0, 0, 0, 0) is an equilibrium point, regardless of the parameters $b_i$, $w_i$, ($i$=1, 2, 3). In order to analyse the characteristic of the equilibrium point (0, 0, 0, 0, 0, 0), the state equation (1) is linearized as

**Table 1.** Equilibrium points $[P_1,\ P_2,\ P_3]$ (where $[\varphi_1,\ \varphi_2,\ \varphi_3] = [0,\ 0,\ 0]$) for different values of parameters $b$ and $w$.

| $b \backslash w$ | 0.3 | 0.5 | 0.7 | 0.9 |
|---|---|---|---|---|
| 0.2 | [0, 0, 0]<br>±[0.8114, –0.5199, –0.5199]<br>±[–0.5199, 0.8114, –0.5199]<br>±[–0.5199, –0.5199, 0.8114] | [0, 0, 0] | [0, 0, 0] | [0, 0, 0] |
| 0.4 | [0, 0, 0] | [0, 0, 0]<br>±[0.6692, –0.3859, –0.3859]<br>±[–0.3859, 0.6692, –0.3859]<br>±[–0.3859, –0.3859, 0.6692] | [0, 0, 0] | [0, 0, 0] |
| 0.6 | [0, 0, 0] | [0, 0, 0] | [0, 0, 0]<br>±[0.5804, –0.3207, –0.3207]<br>±[–0.3207, 0.5804, –0.3207]<br>±[–0.3207, –0.3207, 0.5804] | [0, 0, 0]<br>±[0.8114, –0.5199, –0.5199]<br>±[–0.5199, 0.8114, –0.5199]<br>±[–0.5199, –0.5199, 0.8114] |
| 0.8 | [0, 0, 0] | [0, 0, 0] | [0, 0, 0] | [0, 0, 0]<br>±[0.5191, –0.2803, –0.2803]<br>±[–0.2803, 0.5191, –0.2803]<br>±[–0.2803, –0.2803, 0.5191] |
| 1 | [0, 0, 0] | [0, 0, 0] | [0, 0, 0] | [0, 0, 0] |

$$\delta x = \mathrm{D}f\left(x_0\right) x, \tag{3}$$

where $\delta x = \mathrm{d}x/\mathrm{d}t$, $\mathrm{D}f\left(x\right) = \mathrm{d}f/\mathrm{d}x$, $f$ is the right hand side of state equation (1), $x = (P_1,\ P_2,\ P_3,\ \varphi_1,\ \varphi_2,\ \varphi_3)^{\mathrm{T}}$, $x_0 = (0,\ 0,\ 0,\ 0,\ 0,\ 0)^{\mathrm{T}}$, and

$$\mathrm{D}f\left(x\right) = \begin{bmatrix} F_{11} & 0 & 0 & F_{14} & 0 & 0 \\ F_{21} & w & w & F_{24} & 0 & 0 \\ 0 & F_{32} & 0 & 0 & F_{35} & 0 \\ w & F_{42} & w & 0 & F_{45} & 0 \\ 0 & 0 & F_{53} & 0 & 0 & F_{56} \\ w & w & F_{63} & 0 & 0 & F_{66} \end{bmatrix}, \tag{4}$$

where

$$\begin{aligned}
F_{11} =& 2b\left(1-P_1^2\right)^{-0.5} P_1 \sin\varphi_1, \\
F_{14} =& -2b\left(1-P_1^2\right)^{-0.5} \cos\varphi_1, \\
F_{21} =& -w + 2b\left(1-P_1^2\right)^{-0.5} \\
& \times \left(1 + P_1^2\left(1-P_1^2\right)^{-1}\right) \cos\varphi_1, \\
F_{24} =& -2b\left(1-P_1^2\right)^{-0.5} P_1 \sin\varphi_1, \\
F_{32} =& 2b\left(1-P_2^2\right)^{-0.5} P_2 \sin\varphi_2, \\
F_{35} =& -2b\left(1-P_2^2\right)^{-0.5} \cos\varphi_2, \\
F_{42} =& -w + 2b\left(1-P_2^2\right)^{-0.5} \\
& \times \left(1 + P_2^2\left(1-P_2^2\right)^{-1}\right) \cos\varphi_2, \\
F_{45} =& -2b\left(1-P_2^2\right)^{-0.5} P_2 \sin\varphi_2, \\
F_{53} =& 2b\left(1-P_3^2\right)^{-0.5} P_3 \sin\varphi_3, \\
F_{56} =& -2b\left(1-P_3^2\right)^{-0.5} \cos\varphi_3, \\
F_{63} =& -w + 2b\left(1-P_3^2\right)^{-0.5} \\
& \times \left(1 + P_3^2\left(1-P_3^2\right)^{-1}\right) \cos\varphi_3, \\
F_{66} =& -2b\left(1-P_3^2\right)^{-0.5} P_3 \sin\varphi_3.
\end{aligned}$$

From Eq.(4), we obtain that the eigenvalues of $\mathrm{D}f\left(x_0\right)$ which are

$$\lambda = \begin{bmatrix} \left(-4b^2-2bw\right)^{0.5}, & -\left(-4b^2-2bw\right)^{0.5}, & 2\left(-b^2+bw\right)^{0.5}, \\ -2\left(-b^2+bw\right)^{0.5}, & 2\left(-b^2+bw\right)^{0.5}, & -2\left(-b^2+bw\right)^{0.5} \end{bmatrix}. \tag{5}$$

From Eq.(5), when $b > 0$, $w > 0$, the certainty is $R_{\rm e}(\lambda_i) = 0$, $(i = 1, 2)$, thus the equilibrium point (0, 0, 0, 0, 0, 0) is non-hyperbolic. Moreover, when $w > b$, we get $R_{\rm e}(\lambda_i) > 0$, $(i = 3, 5)$ and $R_{\rm e}(\lambda_i) < 0$, $(i = 4, 6)$ as well, so the equilibrium point is non-stable. Therefore the origin is not structurally stable, and cannot be observed experimentally or in simulations.

## 3.2. Bifurcation and chaotic behaviour

In order to analyse the QCNN's bifurcations and chaotic behaviours, numerical calculation is applied to state equation (1). The bifurcation diagrams, Lyapunov-exponents spectra, Poincaré maps, trajectories, time waveforms, and power spectra are obtained. The QCNN's bifurcations and chaotic behaviours can be found via analysing and contrasting the above simulation figures.

Firstly, we pay attention to the unbalanced cells (different coupling parameters) coupled QCNN. In this case, system parameters are chosen as follows:

$$w_1 = 0.5, \quad w_2 = 0.3, \quad w_3 = 0.2, \quad b_1 = b_2 = b_3 = b.$$

The parameter $b$ is chosen as bifurcation parameter, with its value ranging from 0 to 0.5. The corresponding bifurcation diagram of state $P_1$ versus the parameter $b$ and the Lyapunov-exponents spectrum are obtained as shown in Fig.2. From Fig.2(a), it can be observed that the system response enters into chaos from quasi-period when $b$ decreases, and quasi-period bifurcation occurs as $b = 0.42$. Figure 2 shows that the bifurcation diagram coincides well with the corresponding Lyapunov-exponents spectrum, and that the system has no period window in chaos region, indicating the chaotic behaviour in the QCNN as a robust chaos. Moreover, from the Lyapunov-exponents spectrum shown in Fig.2(b), one can see that the QCNN system is hyper-chaotic when parameter $b$ is in some region because there are two or three positive Lyapunov exponents.

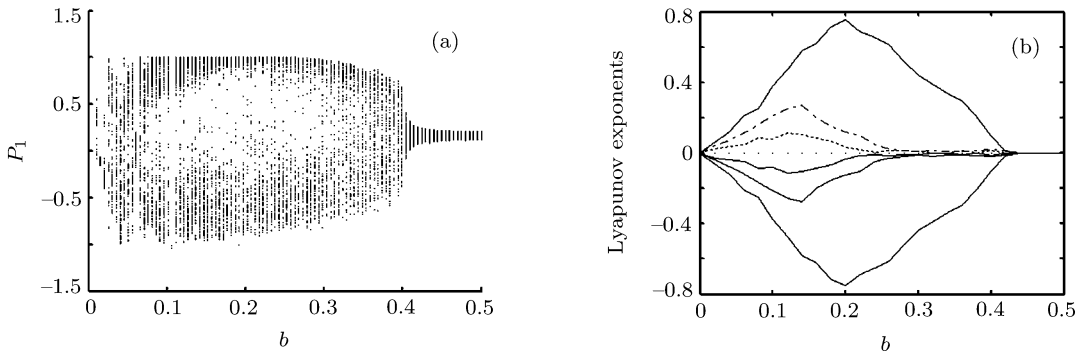



**Fig.2.** (a) Bifurcation diagram of $P_1$ versus $b$ with $b \in [0,\ 0.5]$; (b) Lyapunov exponent spectrum.

When $b = 0.45$ with no other system parameters changed, the system's Poincaré map, trajectory, time waveform, and power spectrum are obtained as shown in Fig.3. Figure 3(a) shows that the Poincaré map is composed of two pieces of thick dots; Fig.3(b) shows that the trajectory is confined to an annular-like region of the state space and is uniformly distributed in this region; Fig.3(c) shows that the time waveform is clearly amplitude-modulated; Fig.3(d) shows that the power spectrum possesses two frequencies. Therefore the system is in quasi-period when $b = 0.45$.

When the parameter $b = 0.28$ is fixed, Fig.4 shows the system's Poincaré map, trajectory, time waveform, and power spectrum. It can be seen that the Poincaré maps are composed of a large number of thick dots distributed over a certain curve, the trajectory exhibits a feature common to many chaotic systems and possesses two strange attractors, the time waveform is similar to random oscillatory waveform, and the power spectrum has a continuous, broad-band nature. Thus the system is chaotic when $b = 0.28$.

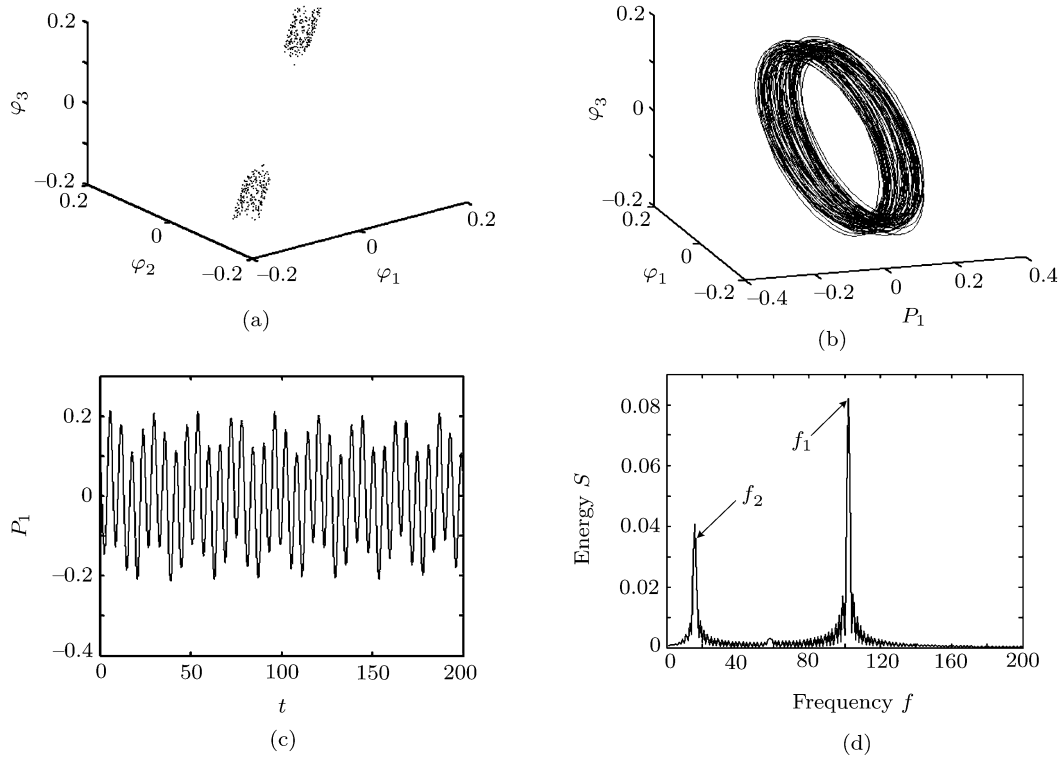



**Fig.3.** A quasi-period solution of the QCNN for $b = 0.45$: (a) Poincaré map; (b) the quasi-period trajectory; (c) the time waveform of $P_1\,(t)$; (d) power spectrum.

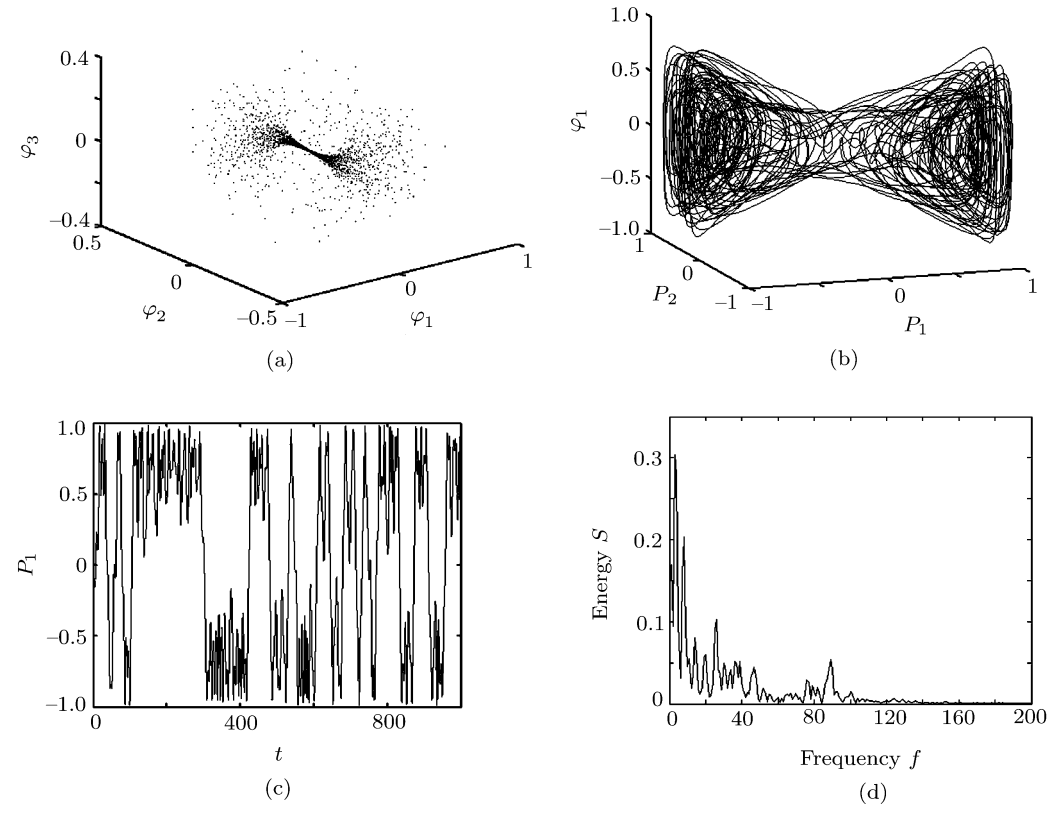



**Fig.4.** A chaotic solution of the QCNN for $b = 0.28$: (a) Poincaré map; (b) the chaotic trajectory; (c) the time waveform of $P_1\,(t)$; (d) power spectrum.

Secondly, we pay attention to the balanced cells (same coupling parameters) coupled QCNN. In this case, system parameters are chosen as follows:

$$w_1 = w_2 = w_3 = w, \quad b_1 = b_2 = b_3 = b.$$

Both the parameters $w$ and $b$ take different values from 0 to 1. The dynamical richness is emphasized in the two-dimensional (2-D) parameters map of Fig.5. In fact, it is remarked that the existence of periodic and quasi-periodic orbits and chaotic and hyper-chaotic attractors.

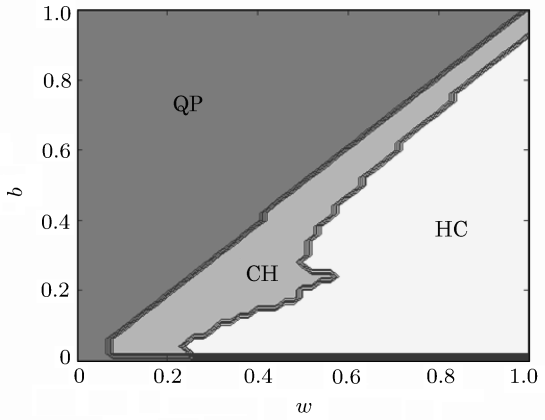



**Fig.5.** 2-D Map of dynamical behaviour of the system for different values of parameters $w$ and $b$ (QP = period or quasi-period, CH = chaos, HC = hyper-chaos).

From Fig.5, it can be found that the balanced cells coupled QCNN also can be chaotic when the parameters are within the range of $w > b$. For example, fixing $w = 0.8$ and varying $b$, we show the bifurcation diagram of state $P_1$ versus the parameter $b$ and the Lyapunov-exponents spectrum in Fig.6, when $b \in [0, 1]$. From Fig.6, it can be observed that the system response enters into chaos from quasi-periodic orbit when $b$ decreases, and quasi-period bifurcation occurs as $b = 0.8$. It also can be observed that the bifurcation diagram coincides well with the corresponding Lyapunov-exponents spectrum, and that the system has no period window in chaos region, indicating the chaotic behaviour in the QCNN as a robust chaos. In addition, from the Lyapunov-exponent spectrum shown in Fig.6(b), one can see that the QCNN system is hyper-chaotic when parameter $b$ is in some region because there are two or three positive Lyapunov exponents.

From the above analysis one can see that it is easy to cause chaotic oscillation in the unbalanced cells coupled QCNN; however, it also can be chaotic when the parameters are within the range of $w > b$ in the balanced cells coupled QCNN. Moreover, both the unbalanced and balanced cells coupled QCNNs can possess hyper-chaotic behaviour.

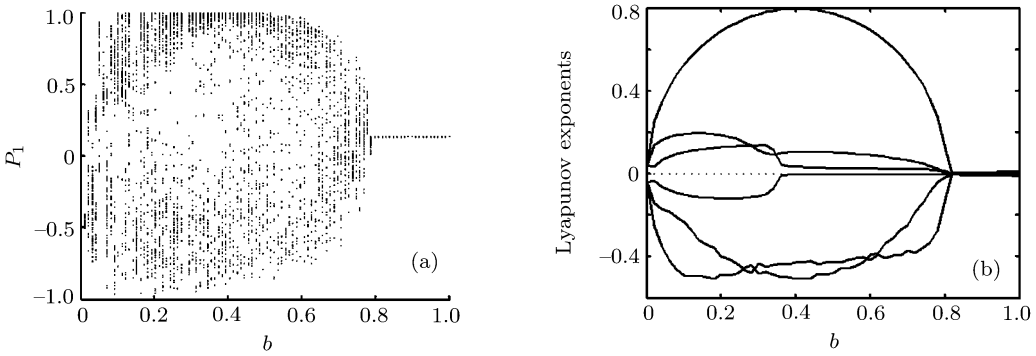



**Fig.6.** (a) Bifurcation diagram of $P_1$ versus $b$ with $w = 0.8$ and $b \in [0, 1]$; (b) Lyapunov-exponent spectrum.

QCNNs possess the advantages of the QCAs and CNNs, whose peculiarities lie in the extremely high packing densities, the extremely low power consumption, and high-parallel signal processing. They represent an innovative architecture for ultra-small realization and massive signal processing. As a very important aspect, they are expected to be used to realize nanometric chaotic generators for control and secure communication in the future.

It must be pointed out that the two stable states with opposite polarization are necessary in quantum computing and classical computing, but it is likely to cause chaotic behaviour in the QCNNs when the coupling parameters of QCNNs are chosen improperly, which will lead to the QCNNs running into an unstable dynamical state. It will make the quantum computing and classical computing produce error. Therefore the coupling parameters of QCNNs should be cho-

sen properly to avoid causing chaotic oscillation when QCNNs are used in quantum computing and classical computing.

## 4. Conclusions

The progressive miniaturization of electronic systems demands for the realization of cellular computing machines in which the cells are in size of the order of nanometres. QCNNs are a very important regime for future evolutions in the field of CNN and, at the same time, in high-parallel signal processing. For one thing, QCNNs may provide a technological improvement suggesting nanometric realizations for CNN, for another, a hardware like CNN circuit still in development could be adopted as an useful platform for high-parallel signal processing.

This paper studies the complicated chaotic dynamical behaviour of a three-cell coupled QCNN, including equilibrium points, bifurcation diagrams, Lyapunov-exponents spectra, Poincaré maps, trajectories, time waveforms and so on. Different phenomena, such as quasi-periodic, chaotic, and hyper-chaotic states as well as bifurcations are revealed. Through the theoretical analysis and practical numerical calculation, we find that the equilibrium points are symmetric and the origin is a non-hyperbolic equilibrium point, so it is not structurally stable. In addition, the unbalanced cells coupled QCNN is easy to cause chaotic oscillation and the system response enters into chaotic state from quasi-periodic state by quasi-period bifurcation, and moreover, the system has no period window in chaos region, indicating the chaotic behaviour in the QCNN as a robust chaos; however, the balanced cells coupled QCNN also can be chaotic when the parameters are within the range of $w > b$. Additionally, both the unbalanced and balanced cells coupled QCNNs can possess hyper-chaotic behaviour.

Thus on the one hand, we should choose adequate coupling parameters to avoid causing chaotic oscillation when QCNNs are used in high-parallel signal processing such as image processing and pattern recognition because chaotic oscillation will lead to QCNNs running into an uncertainly dynamical state; on the other hand we can employ QCNNs with given coupled parameters to realize novel ultra-small chaotic generators for control, synchronization, and secure communication, and moreover these chaotic generators will possess very simple structures in which few cells are employed.

## References


[1] Snider G L, Orlov A O, Amlani I, Zuo X, Bernstein G H, Lent C S, Merz J L and Porod W 1999 *J. Appl. Phys.* **85** 4283

[2] Lent C S, Tougaw P D, Porod W and Bernstein G H 1993 *Nanotechnology* **4** 49

[3] Lent C S and Isaksen B 2003 *IEEE Transactions on Electron Devices.* **50** 1890

[4] Wang C K, Gao T J and Xue C S 2000 *Acta Phys. Sin.* **49** 2033 (in Chinese)

[5] Kim K, Wu K and Karri R 2007 *IEEE Transactions on Computer-Aided Design of Integrated Circuits and Systems* **26** 176

[6] Wang S, Cai L and Guo L 2005 *Research and Progress of Solid State Electronics* **25** 148 (in Chinese)

[7] Wang S and Cai L 2007 *Solid State Phenomena* **121** 565

[8] Tóth G, Lent C S, Tougaw P D, Brazhnik Y, Weng W, Porod W, Liu R W and Huang Y F 1996 *Superlattices and Microstructures* **20** 473

[9] Civalleri P P and Gilli M 2004 *Int. J. Circuit Theory and Application* **32** 79

[10] Cai L, Ma X K and Wang S 2003 *Acta Phys. Sin.* **52** 3002 (in Chinese)

[11] Wang S, Cai L and Liu H C 2005 *J. Air Force Engineering University* (Natural Science Edition) **6** 85 (in Chinese)

[12] Wang S, Cai L, Li Q and Wu G 2007 *Chin. Phys.* **16** 2631

[13] Chua L O and Yang L 1998 *IEEE Tran. Circuit Sys.* **35** 1257

[14] Porod W 1997 *J. Franklin Inst.* **334B** 1147

[15] Ma X K, Yang M, Zou J L and Wang L T 2006 *Acta Phys. Sin.* **55** 5648 (in Chinese)

[16] Wang G Y, Liu J B and Zheng X 2007 *Chin. Phys.* **16** 2278

[17] Wang X Y and Wang M J 2007 *Acta Phys. Sin.* **56** 5136 (in Chinese)